6ICEGE 6th International Conference on Earthquake Geotechnical Engineering
1-4 November 2015
Christchurch, New Zealand

Numerical Analysis for Seismically-Induced Deformations in Strain-Softening Plastic Soils

M.H. Beaty[1], S.E. Dickenson[2]

ABSTRACT

Embankments and slopes with saturated clays and plastic silts are subject to large deformations during earthquakes, particularly when these soils are normally consolidated or lightly over-consolidated. Shear strains accumulate through cyclic softening. The undrained strength may also decrease through progressive remolding. Modeling this behavior in an analysis is challenging for a number of reasons, including 1) the limited strains achieved in typical laboratory tests, 2) differences between field and laboratory behavior due to strain localization, 3) strain rate effects, and d) dependence of strain estimates on numerical mesh density. The impact of these challenges on the reliability of analysis results is uncertain. An evaluation of an analysis approach is made through a back-analysis of the 4th Avenue Landslide during the 1964 M 9.2 Alaskan Earthquake. Key aspects and uncertainties in the deformation analysis are identified, and recommendations for practice are made.

Introduction

One of the most significant impacts of the 1964 Great Alaskan Earthquake in the City of Anchorage was the initiation of large landslides. One slide along 4th Avenue was about 490m long, 275m wide, and moved horizontally up to 5.8m with the formation of grabens behind and between the slide masses. Vertical offsets associated with the grabens approached 3.3m. The likely failure mechanism of this slide involved seismically-induced undrained strength loss within the lightly overconsolidated Bootlegger Cove Clay (BCC) layer (Idriss, 1985).

Seismic analyses that include clay-like soils with both cyclic softening and significant strength loss are a particular challenge. The 4th Avenue slide provides a valuable case history for assessing numerical analysis techniques and identifying key factors: the soil strata at the slide are relatively simple, the failure mechanism is well understood, and there are ample records of the observed displacements. The objectives of this back-analysis are to evaluate the influence of key input parameters on computed deformations through parametric study and to develop guidance for numerical analysis.

Geotechnical Characterization

The representative cross-section for the analysis is shown on Figure 1 and is a simplified version of the one developed by Shannon and Wilson (1964). This section represents the western third of the slide and is characterized using 5 soil units. The descriptions for each unit were based primarily on information from Shannon and Wilson (1964), Idriss (1985), Stark and Contreras (1998), Boulanger and Idriss (2004), and Port of Anchorage (2015).

[1]Principal Engineer, Beaty Engineering LLC, Beaverton, Oregon, USA, mhb@beatyeng.com
[2]Principal Engineer, New Albion Engineering Inc., Reno, Nevada, USA, sed@newalbiongeotechnical.com

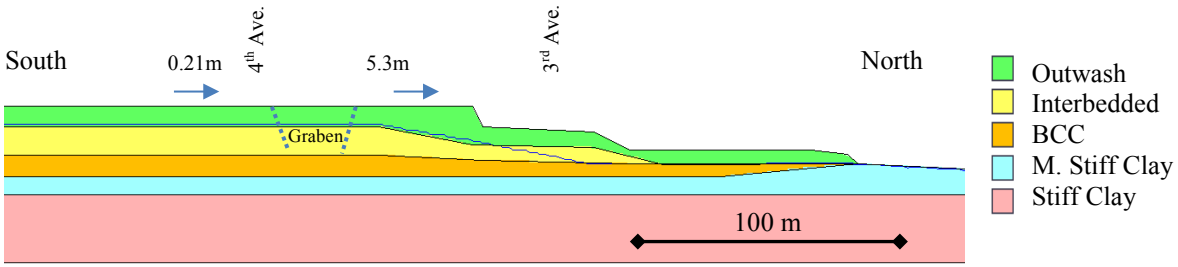

Figure 1. Cross-section along D Street as incorporated in FLAC analysis.

Seven facies of BCC have been described to indicate differences in depositional environment and post-depositional modification. The critical BCC layer at 4th Avenue belongs to facies III, which is noted for its sensitivity. The adopted strengths for the BCC layer are based on direct simple shear (DSS) tests and constant volume ring shear tests. The peak undrained strength ratio (S_u/σ'_{vo}) versus OCR are shown on Figure 2a. The OCR near the top of the BCC layer was estimated to be about 1.2 for the upper portions of the slide. A relationship between pre-consolidation pressure and elevation was then developed assuming the site was originally uniform and level. The OCR in the BCC increases as the ground surface drops, reaching a maximum estimated value of about 3 at the northern end. The S_u assigned to each element was developed from the relationship on Figure 2a and the corresponding estimate of OCR. A residual strength ratio (S_r/σ'_{vo}) of 0.06 was developed from ring shear tests (Stark and Contreras, 1998). The measured PI averages about 14 with a range of 7 to 22. A drained friction angle of 30° and a unit weight of 19 kN/m^3 were used.

The Outwash layer consists of very dense sands and gravels deposited by streams from retreating glaciers. This layer is 7.5m to 12m thick. A friction angle of 38° and a unit weight of 20.4 kN/m^3 were assumed. A modest increase in shear strength near the surface was used to stabilize the existing steep slopes in the analysis. The Interbedded zone is a layered deposit of stiff BCC that includes cohesionless soil layers that are often thin and appear to be discontinuous. The cohesionless soils are dense to very dense silty fine sand and sandy silt. The clay layers have overconsolidation ratios (OCR) of 3 to 4. Both the Interbedded and BCC formations were deposited in a proglacial lake. A friction angle of 35° and a unit weight of 20.0 kN/m^3 were assumed for the Interbedded zone. The undrained strengths assigned to the medium stiff and stiff clay units were selected to minimize plastic failure during the earthquake. These zones were assumed to be sufficiently over-consolidated to prevent significant yielding. A unit weight of 20.4 kN/m^3 was assumed.

The shear wave velocity (V_S) adopted for the analysis is shown on Figure 2b. This profile was approximated from the local soil strata and measured V_S values at two nearby locations: site C-6 is about 1500m east of the 4th Avenue slide and site C-7 is about 450m south and west (Nath et al., 1997). The 4th Avenue profile is also in reasonable agreement with the V_{S30} contours proposed by Dutta et al. (2000). While the adopted profile is considered a reasonable estimate of likely conditions, the V_S at depth is less certain. A half-space with a V_S of 500 m/s was assumed for the analysis based on the measurements from C-6 and C-7.

The modulus reduction and damping characteristics were approximated from published relationships. Cohesionless zones were assumed to follow the depth-dependent recommendations from EPRI (1993), while the relationships of Vucetic and Dobry (1991) for clay with PI=15 were assumed for the BCC and stiff clays.

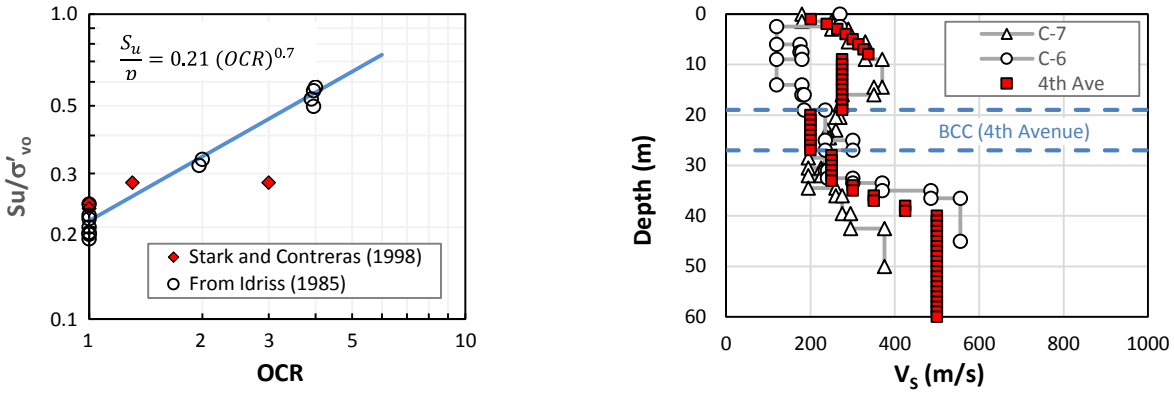

a) Undrained strength of BCC

b) Shear wave velocity profile.

Figure 2. Undrained strength and V_s profiles for analysis.

Analysis

The analyses were performed using the 2D finite difference program FLAC 7 (Itasca, 2011). The numerical model represents a section that is 750m long and up to 60m deep. Free-field boundaries were used at the lateral edges and a compliant boundary at the base during the seismic analysis. The typical element height in the BCC was 0.66 m.

Constitutive Models

A practice-oriented hysteretic model (Hyper-U) was used to simulate the cyclic behavior of the soils. Hyper-U is a non-linear stress strain model that simulates the effects of pore pressure generation, softening due to reduction in effective stress, and strength loss with accumulated strain. It is similar to the model described in Stark et al. (2012). Model parameters were adjusted to reasonably match the target modulus and damping curves as shown on Figure 3. Rayleigh viscous damping was also used (1% at 1.2 Hz).

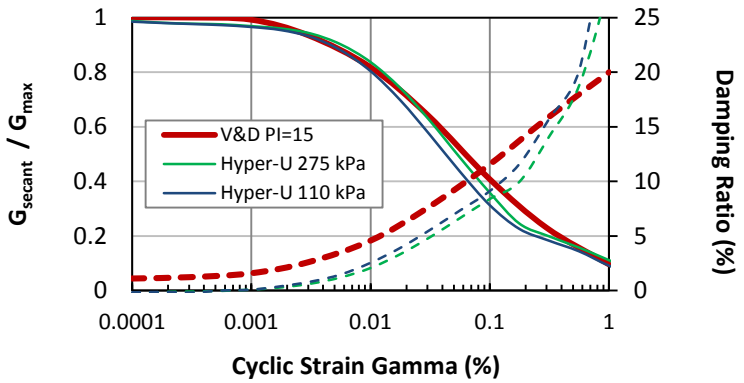

Figure 3. Modulus reduction and damping behavior for BCC.

Cyclic tests on BCC were used to guide the calibration of Hyper-U: tests by Lade et al. (1985) on samples representative of downtown Anchorage and tests from the Port of Anchorage (2015). These tests were performed on samples of facies I, II, and IV of the BCC. The cyclic strengths from each test were normalized by the undrained strength as shown on Figure 4a. Although the cyclic behavior of each facies may differ, the trend line after normalization was considered a reasonable starting point for the parametric analyses. The Lade et al. results are somewhat uncertain as the S_u values were approximated.

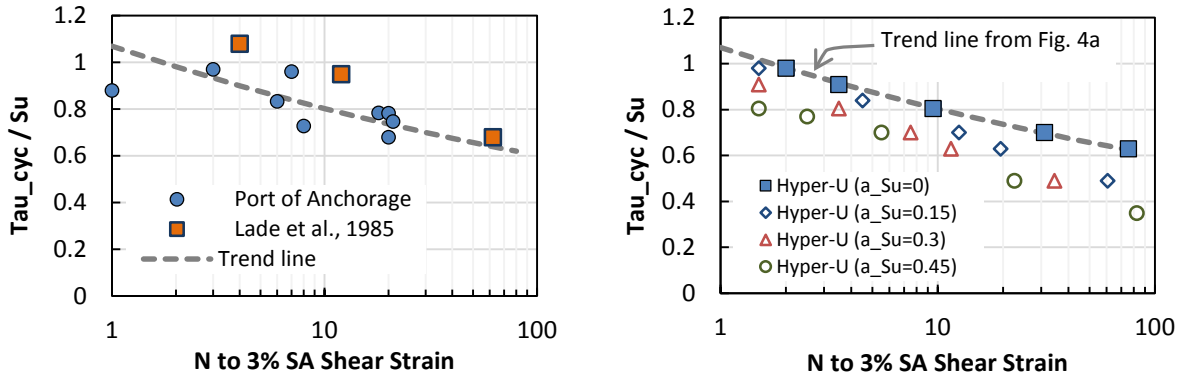

a) Cyclic test results for $\alpha\_S_u=0$ b) Hyper-U Calibration

Figure 4. Cyclic strength behavior of BCC.

Figure 4b compares the calibrated Hyper-U behavior for σ'_{vc}=275 kPa and OCR=1.2 (blue squares) with the trend line from Figure 4a. Simulations were also performed for values of α_S_u equal to 0.15, 0.3, and 0.45, where α_S_u is defined as the initial static shear stress divided by S_u. Hyper-U shows decreasing cyclic resistance with increasing α_S_u. Values of α_S_u are generally less than 0.30 in the FLAC analyses, with limited areas up to 0.45.

The S_u of the BCC was adjusted for strain rate effects during seismic loading. A strain rate factor (SRF) of 1.4 was applied to the static S_u for both calibration and analysis to approximate the available strength at a loading frequency of about 1 Hz. (Note: an SRF of 1.4 was also applied to the Interbedded zone, although some preliminary analyses reported below used an SRF of 1.0). The strain-softening behavior of BCC was also included by making S_u a function of the maximum shear strain (γ). The available ring shear tests provide information on both the magnitude and rate of strength loss, but the relationships between ring shear displacement, field displacement, and shear strain estimates are uncertain. The function between S_u and γ to be used for any particular analysis requires judgment. Reasonable trial functions for these analyses were developed from available information as discussed below.

A key observation from the 4th Avenue slide concerns the distribution of ground surface displacements: horizontal movements tended to be less than 0.15m or greater than about 3m (Idriss, 1985). This suggests S_u began degrading at some surface displacement less than 0.15m. If we make several assumptions (i.e., the strength did not degrade until the displacement reached 0.15m, little strain localization occurred until pronounced strain softening, and the ground displacement was due solely to strains within the BCC), then the average γ in the BCC at the start of strength degradation was only about 2%. This seems unlikely and suggests some localization within the BCC, perhaps due to strength variations in sublayers. However, a numerical analysis may estimate a relatively uniform distribution of shear strain across this layer at small surface displacements. This suggests the analysis may need to initiate strength degradation at relatively small values of γ (i.e., < 2 to 4%).

Newmark-type analyses were performed by Stark and Contreras (1998) to estimate a relationship between surface displacement and mobilized strength. These analyses suggested that surface displacements would be less than about 0.15m if at least 80% of S_u was maintained along the failure plane. Since S_u has been increased by a factor of 1.4 for strain rate in the FLAC analyses, this equates to an equivalent strength loss of up to 0.8/1.4 = 57% for displacements of about 0.15m.

Stark and Contreras also estimated that S_r was mobilized at a surface displacement of about 2.5m. Due to localization, much of this displacement would likely occur in the FLAC analysis through shear strains in a single row of elements. This suggests that S_r should be fully mobilized in the analysis at shear strains on the order of 2.5/0.66 ≈ 400%. Considering the shape of the S_u versus displacement curves from the ring shear tests, four trial relationships for strain-softening factor versus γ (labeled SF #1 to SF #4) were defined as shown on Figure 5. The softening factor is applied using the equation shown on Figure 5. S_u begins to degrade at γ = 2% for all 4 curves. The most abrupt softening (SF #1) assumes full strength loss at γ=10%, while the most gradual curve (SF #4) assumes full softening at γ=240%. The strain-softening relationships were used only for the BCC unit.

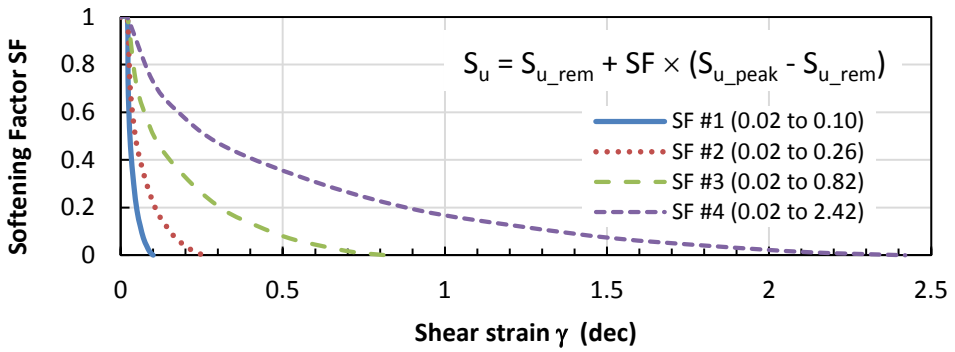

Figure 5. Strain-softening relationships used in parametric study.

Earthquake Loading

The hypocenter of the 1964 earthquake was about 120 km from Anchorage. Although motions were not recorded locally, the PGA near the slide was estimated at 0.15g to 0.2g with 2 to 3 minutes of strong shaking (Idriss, 1985). Sliding at 4th Avenue reportedly began about 1.5 minutes after the start of shaking and stopped at the end of shaking.

The input ground motions were developed considering estimates of the response spectrum. The four GMPEs and weighting factors adopted by the USGS for the 2014 NSHMP were used for this study (USGS, 2014). Two target spectra were developed: one for the ground surface (V_{S30} = 250 m/s) and one for the halfspace (V_{S30} = 500 m/s). An ε of 0.38 was required to achieve a PGA of 0.18g at the ground surface, where ε is the number of standard deviations added to the mean estimate. This same ε was then used to estimate the response spectrum for the half space.

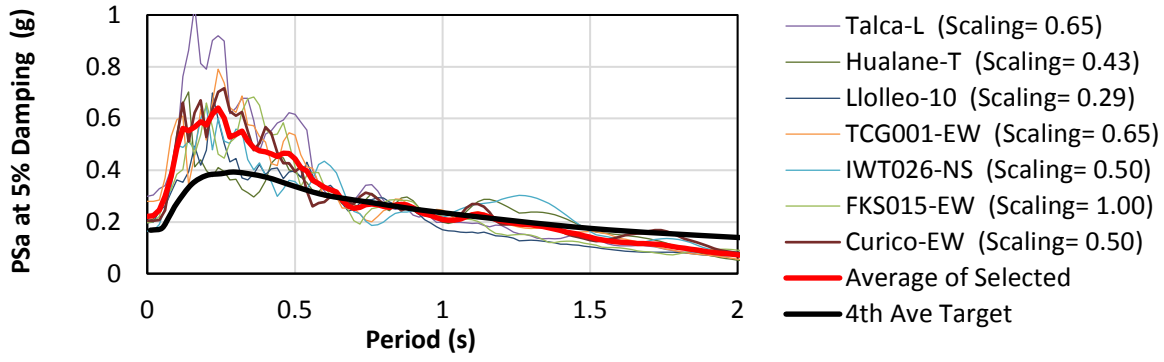

Figure 6. Response spectra of scaled earthquake records.

Seven ground motion recordings were selected from historic subduction earthquakes: 1985 Valparaiso M_w=7.8, 2010 Maule M_w=8.8, and 2011 Tohoku M_w=9 (NIED, 2015). The records were linearly scaled to the target spectrum over the frequency range of interest. The fundamental period at the south end of the section is about 0.6 seconds for small strain conditions. The scaled spectra are shown on Figure 6. The corresponding vertical motions were also used in the analysis with the same scaling factor.

Parametric Study

An example of the displacements estimated in the parametric study is shown on Figure 7. The pattern, magnitude and timing of the displacements from this example are generally consistent with observations. Significant displacements did not begin until about 70 s after the start of shaking. One clear difference between the observed and estimated response is the lack of graben formation in the analysis. This may be related to the assumption of no strength degradation with strain in the Outwash and Interbedded zones and will be investigated in future analyses. Significant vertical displacements were also estimated behind the top of the slope. This suggests an exaggerated rotational component in the analysis. Pressure bulging up to 0.9m is estimated on the lower bench which generally corresponds to observations.

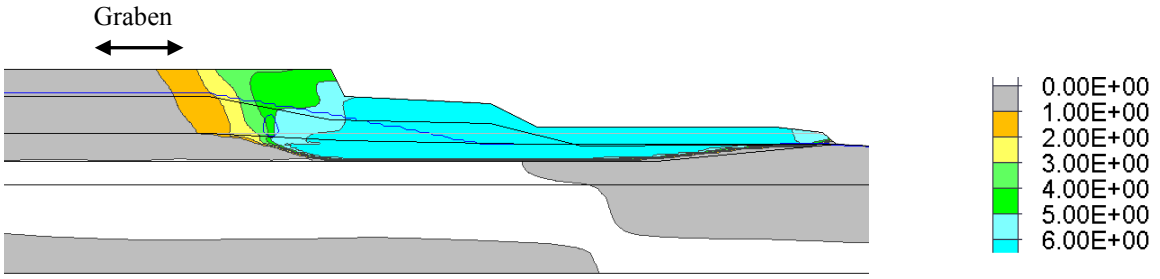

a) Horizontal displacements in meters.

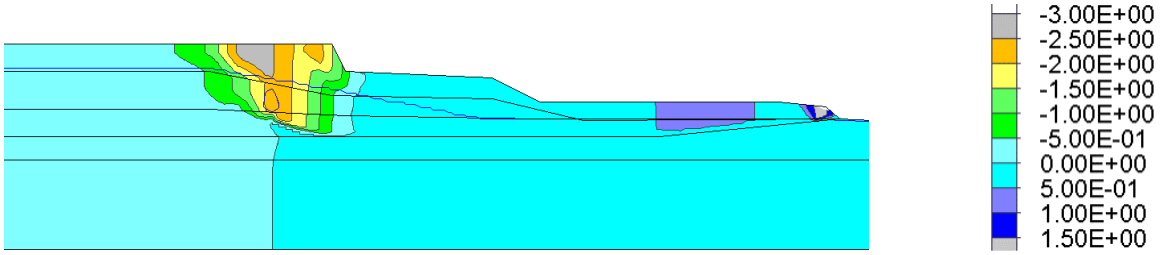

b) Vertical displacements in meters.

Figure 7. Example displacement contours from FLAC analyses.

Input motions with larger amplitudes than shown on Figure 6 were required to induce the observed displacement magnitudes in the parametric study. An additional scaling factor of 1.4 was applied to the input motions for these analyses. Significant deamplification of the input motion was estimated with an average ground surface PGA estimate behind the slide of about 0.21g. A dependence between the amplitude of the surface motion and slide displacement was also found as shown on Figure 8a. Note that PGA in this context is used only as a proxy for the amplitude of response from the selected input motion. This figure also suggests the input motions needed to produce a PGA of at least 0.15g to generate significant slide displacements.

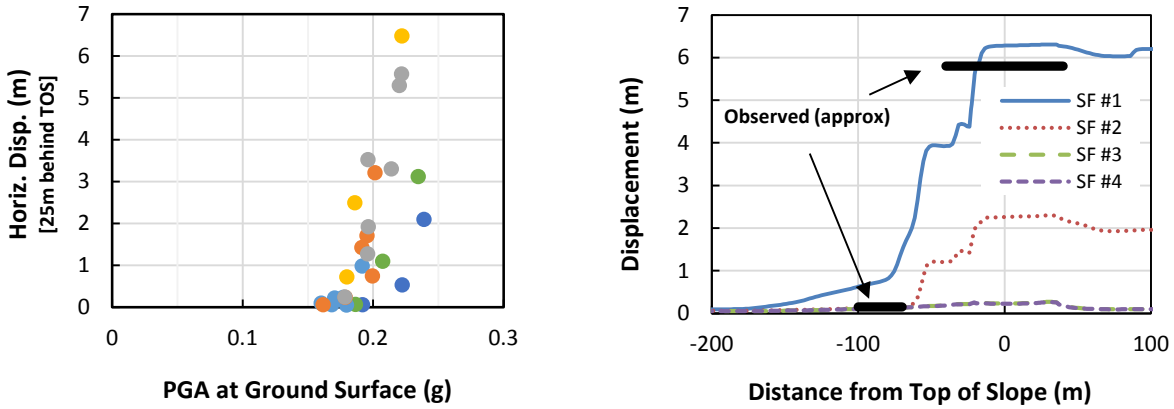

a) Estimated displacements (m) b) Effect of strain-softening factor

Figure 8. Horizontal surface displacements from parametric studies.

Figure 8b presents examples of estimated surface displacements as a function of the assumed strain-softening relationship. The most abrupt softening relationship (SF #1 as shown on Figure 5) was required to produce displacement magnitudes similar to those observed. This is a significant finding as SF #1 is much different than typically estimated from test results. The importance of the adopted softening relationship was further suggested from an analysis using a finer mesh along with the SF #1 relationship and the Talca-L motion. The element height and width were reduced by a factor of 2 in the BCC, which produced an increase in horizontal displacement of the slide mass of about 50%.

The importance of strain rate factor on estimated displacements was evaluated by analyzing cases with different SRF values. Reducing the SRF from 1.4 to 1.3 resulted in a 50% increase in displacements, while using SRF=1.2 caused a fourfold increase. Incorporating strain rate factors is key to obtaining reasonable response estimates. The potential effect of strain localization on strain rate, and the corresponding influence on S_u and cyclic resistance, is a further complication to the analysis of strain-softening soils that was not evaluated.

Conclusions

An analytical study of the 4th Avenue slide and its response to the 1964 Great Alaskan Earthquake was performed to identify challenges in modeling plastic soils subject to cyclic softening and strength loss. The analysis approach used the computer program FLAC along with a practice-oriented, non-linear constitutive model for the sensitive clay.

The estimated magnitude and pattern of displacements were found to be highly dependent on the relationship of strength versus shear strain adopted to characterize strain softening. The best displacement estimates were obtained when strength loss occurred abruptly and at relatively low values of shear strain (e.g., between γ=2% and γ=10%). These strains are less than suggested by laboratory tests but they do not necessarily reflect peak strains in the soil: FLAC provides estimates of average strain over the height of each element. Any shear localization that occurs at scales less than the element dimension will not be directly estimated. An analysis using a refined mesh in the BCC further demonstrated the link between the required strain-softening relationship and the size of the numerical element.

The current analyses results are preliminary. They represent an evolving study with continuing refinements in the input parameters. However, they are considered sufficient to support several initial recommendations for seismic deformation analyses of sensitive soils using similar analysis approaches. Calibration of the constitutive model for strain softening, when used with typical grid element sizes, may need to consider a relatively abrupt loss of strength at small average strains. Thorough parametric studies, including element size effects, should be performed due to the dependence of deformations on uncertain asumptions on strain softening. In addition, one of the key observations from the 4th Avenue slide was the onset of large deformations once surface displacements exceeded about 0.15m. This observation provides a valuable check to analyses involving similar materials and geometries.

References

Boulanger, R.W., and Idriss, I.M. *Evaluating the Potential for Liquefaction or Cyclic Failure of Silts and Clays*. UC Davis, Center for Geotechnical Modeling, Report No. UCD/CGM-04/01, 2004.

Dutta, U., Biswas, N., Martirosyan, A., Nath, S., Dravinski, M., Papageorgiou, A., and Combellick, R. Delineation of spatial variation of shear wave velocity with high-frequency Rayleigh waves in Anchorage, Alaska. *Geophys. J. Int. 2000;* **143**: 365-375.

EPRI. *Guidelines for Site Specific Ground Motions*. Palo Alto, CA. Electrical Power Research Institute, November-TR-102293, 1993.

Hansen, W.R. *The Alaska Earthquake, March 27, 1964 -- Effects on Communities*. Geological Survey Professional Paper 542-A, US Dept. of the Interior, Geological Survey, 1965.

Idriss, I.M. Evaluating Seismic Risk in Engineering Practice. *Proc. 11th Int. Conf. on Soil Mech. and Found. Eng., San Francisco, California, 1985*. Theme paper. 255-320.

Itasca. *FLAC, Fast Lagrangian Analysis of Continua, Version 7.0.* Itasca Consulting Group, Minneapolis, MN, 2011. http://www.itascacg.com/

NIED. *Strong-motion Seismograph Networks (K-NET, KiK-net).* National Research Institute for Earth Science and Disaster Prevention, 2014. http://www.kyoshin.bosai.go.jp/

Nath, S.K., Chatterjee, D., Biswas, N.N., Dravinski, M., Cole, D.A., Papageorgiou, A., Rodriguez, J.A., and Poran, C.J. Correlation Study of Shear Wave Velocity in Near Surface Geological Formations in Anchorage, Alaska. *Earthquake Spectra 1997*; **13**(1): 55-75.

Port of Anchorage. Project reports provided by the Port of Anchorage for the Intermodal Expansion (Marine Terminal Redevelopment), 2015.

Shannon and Wilson, Inc. *Report on Anchorage area soil studies, Alaska, prepared for USACE District, Anchorage, Alaska*. Contract No. DA-95-507-CIVENG-64-18, 1964.

Stark, T.D., Beaty, M.H., Byrne, P.M., Castro, G.V., Walberg, F.C., Perlea, V.G., Axtell, P.J., Dillon, J.C., Empson, W.B., and Mathews, D.L. Seismic Deformation Analysis of Tuttle Creek Dam. *Canadian Geotechnical Journal 2012*; **49**(3): 323-343.

Stark, T.D. and Contreras, I.A. Fourth Avenue Landslide during 1964 Alaskan Earthquake. *ASCE J. Geo. And Geoenv. Eng. 1998;* **124**(2): 98-109.

USGS. *Documentation for the 2014 Update of the United States National Seismic Hazard Maps*. Open-File Report 2014-1091, 2014. http://pubs.usgs.gov/of/2014/1091/.

Vucetic, M. and Dobry, R. Effect of Soil Plasticity on Cyclic Response. *ASCE J. Geot. Eng. Div. 1991*, **117**(1): 89-107.